

Key Ingredients for Superconductivity in Cuprates

Z. -X. Shen¹, A. Lanzara^{1,2} and N. Nagaosa³

¹*Department of Physics, Applied Physics and Stanford Synchrotron Radiation Lab., Stanford University, CA 94305*

²*Advanced Light Source, Lawrence Berkeley National Lab., Berkeley, CA 94720*

³*Department of Applied Physics, University of Tokyo, Bunkyo-ku, Tokyo 113, Japan*

(January 30, 2020)

Using high resolution angle-resolved photoemission data in conjunction with that from neutron, optics and local structural probes, we show that electron-phonon (el-ph) coupling is strong in cuprate superconductors and it plays an important role in pairing. The inclusion of phonons provides a theoretical framework explaining many important phenomena that cannot be understood by a strongly correlated electronic model alone. The el-ph coupling is investigated in the context of strongly interacting electron system and is found to be helpful for d-wave pairing.

PACS numbers: 79.60.Bm, 73.20.Dx, 74.72.-h

It has been a long-standing question whether a strongly correlated electronic model of the CuO₂ plane, such as the t-J or Hubbard model alone, can explain the essential experimental observation of superconductivity in cuprate oxides. On the one hand, such a model has been remarkably successful in explaining many important physical properties, most notably the property of the undoped insulator and the renormalization of charge dynamics in it, by spin dynamics from t to J scale^{1,2} and in predicting a spin gap^{3,4}. On the other hand, important questions have been raised. The first is the observation that, while the CuO₂ plane conductivity is essentially the same for various families of cuprates, their T_c varies by at least an order of magnitude^{5,6}. The second is the observation that the phonons and lattice effects are clearly present in these materials⁷, following the original assumption that the Jahn-Teller (JT) polarons might be important for superconductivity⁸. There is currently no consensus on the above issues.

This paper addresses these problems by providing experimental evidence pointing toward phonon to be also an essential player: (i) the phonon strongly influences the electronic dispersion, (ii) the strength of the el-ph coupling correlates with that of pairing. These finding suggests that both electron-electron (el-el) and el-ph interactions are essentials ingredients for superconductivity in cuprates.

Fig. 1a summarize the systematics in the superconducting gap size (Δ), together with the transition temperature (T_c) shown in Fig. 1c. Unlike T_c, which can be depressed by phase fluctuations in the underdoped regime⁹⁻¹¹, the superconducting gap essentially reflects the pairing strength. It can be clearly seen that the pairing strength for the p-type cuprates is very strong, with gap sizes that are at least an order of magnitude larger than conventional superconductors. Further, the maximum T_c of each family is controlled by the maximum superconducting gap size. This is most dramatically illustrated by the HgBa₂Ca_{n-1}Cu_nO_{2(n+1)} (Hg1223 for n=3) compound, which has a much larger gap size as well as

T_c. Fig 1a also clearly shows a discrepancy between p- and n- type materials, as superconductivity in a n-type material appears to be very fragile with a much weaker pairing strength.

In a strong coupling conventional superconductor the superconducting transition temperature is

$$T_c = \frac{\omega_0}{1.45} \exp \left[\frac{-1.04(1+\lambda)}{\lambda - \mu^*(1+0.62\lambda)} \right] \quad (1)$$

where the notations are standard¹². For T_c to increase, one in principle should increase the phonon frequency ω_0 . This, unfortunately, leads to two problems. The first is the Coulomb repulsion $\mu^* = \mu/(1 + \mu \ln(E_F/\omega_0))$, which increases rapidly with increasing ω_0 , since the retardation effect is less effective. The second is that higher frequency means smaller λ , because $\lambda = C/M\omega_0^2$, where C is a constant for a given class of materials. In order to have a large λ , as well as high ω_0 , one has to increase the constant C, which often leads to structural phase transitions. These two factors conspire to limit the value of T_c in conventional superconductors. The values shown in Fig. 1 for cuprates make it clear that the conventional wisdom with phonons will not be able to generate the observed gap size, and thus T_c.

Recent high-resolution angle-resolved photoemission (ARPES) data however, suggest that phonons may nevertheless be an essential player. By analyzing photoemission data from Bi₂Sr₂CaCuO₈ (Bi2212), Bi₂Sr₂CuO₆ (Bi2201) and La_{2-x}Sr_xCuO₄ (LSCO), in addition to earlier data from Bi2212¹³⁻¹⁵, we concluded that the quasiparticles in p-type cuprates are strongly coupled to phonons in the frequency range 50-80meV¹⁶, in contrast to that of the n-type material¹⁷. We see a dramatic change in the "quasiparticle" velocity in the form of a break in the dispersion near this energy scale, as shown in Fig. 2 (a-c) where the dispersion along the nodal direction for three families of p-type cuprates are plotted. This result is very robust, and the details of the fit can be found elsewhere^{14,16}. This effect gets stronger as one

moves towards other directions of the zone, by a factor of two to three towards $(0,0)$ to $(\pi,0)$ direction. In related data, a clear drop in the quasiparticle scattering rate below this energy scale is observed^{14,15}, which is consistent with optics data reporting a rapid drop of the scattering rate, $1/\tau$, at similar energy¹⁸. The fact that both photoemission and optics see the same effect in scattering rate, gives great confidence to this observation. The observed behavior, a sudden change in the dispersion and a drop in the scattering rate, is very reminiscent of quasiparticle coupled to a sharp collective mode. The famous 41 meV neutron mode and phonons are the only two sharp collective modes we are aware of. Since this effect is seen in all compounds and is not associated with the superconducting phase, as the phenomena are seen well above T_c , we rule out the neutron mode possibility¹⁹, as neutron modes are only seen in $\text{YBa}_2\text{Cu}_3\text{O}_{7-x}$ (YBCO) and Bi2212 and are only associated with superconductivity. We note here that the Bi2201 data was collected at 30K, six times higher than T_c . Alternatively one may try to explain the data by the opening of a gap elsewhere on the Fermi surface. However, the superconducting and pseudogap in LSCO, Bi2201 and Bi2212 are very different, but the "kink" energy is very similar, so this explanation does not work. Thus we are left with phonons as the only surviving candidate to explain our data¹⁶.

The phonon interpretation receives additional support from comparison between photoemission and neutron data. Neutron scattering data from LSCO and YBCO suggest that a particular zone boundary phonon couples most strongly to doped charge²⁰ and softens significantly with doping. In the case of LSCO, where a direct comparison between neutron and photoemission is possible, the phonon mode appears at 70meV. As shown by the thick arrow in Fig. 2c, the phonon energy coincides with the "kink" energy in the dispersion, providing a very strong piece of direct evidence for the phonon being the mode responsible for the effect seen in quasiparticle dynamics. In a separate analysis we compare the dip position of the famous "peak-dip-hump" structure in the EDC of Bi2212 and find the energy scale to be close to that of the phonon energy in YBCO and Bi2212¹⁶. This again is consistent with the phonon interpretation, as a phonon mode will cause a dip in the spectral function^{12,21}. In a gapless superconductor the dip energy has its lower bound near the phonon frequency. In summary, we believe that this ensemble of data makes a compelling case for a strong coupling between quasiparticles and phonons.

In conventional theory the phonon correction to the electronic velocity is given by $v(k) = v_0/(1+\lambda')$, where v_0 is the bare electron velocity (below the phonon frequency ω_0), $v(k)$ is the dressed velocity (above the phonon frequency) and λ' is proportional to the el-ph coupling constant²². Adopting a similar approach we find that the velocity ratio of p-type materials is close to two near optimal doping and increases with underdoping. While the correlation effect and strong coupling may modify things, we think that the el-ph coupling constant near

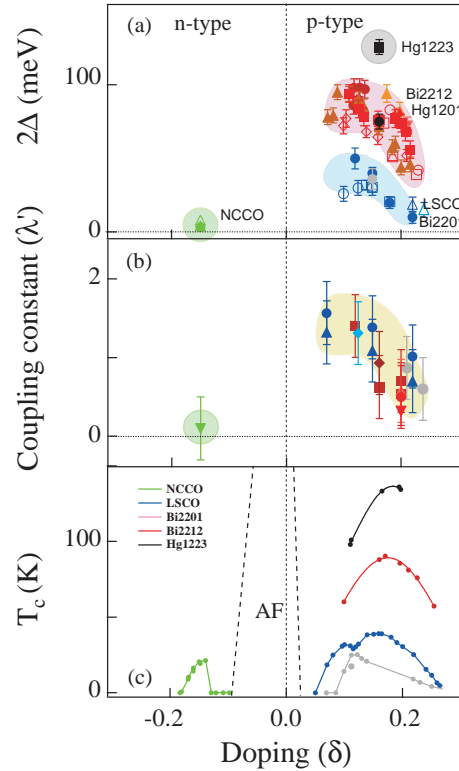


FIG. 1. In panel (a) we plot the superconducting gap determined by photoemission spectroscopy (full symbol)⁵³ and tunneling spectroscopy (empty symbols)⁵⁴ as reported in the literature as well as determined from our data. In panel b) the doping dependence of the coupling constant is reported for LSCO, Bi2201 and Bi2212 (right side) and NCCO (left side) as determined by angle resolved photoemission, along the nodal direction ($\Gamma - Y$). In panel (c) (right side), we report the doping dependence of the critical temperature for four different p-type systems: Hg1223, Bi2212, Bi2201 and LSCO as reported in the literature⁵⁵. On the left side of the same panel, we report the critical temperature for the NCCO⁵⁵. The shaded area are a guide to the eyes.

optimum doping is larger than one, indicating a strong coupling. The el-ph coupling constant (λ') as a function of doping is plotted in Fig 1b. We note that the frequency scale of the phonon here is an order of magnitude higher than that of conventional superconductors. In principle, given the high λ' value, it can deliver a pairing strength that is an order of magnitude higher with respect to the conventional superconductors, if one can figure out a way to deal with the μ^* problem. As we will elaborate later, the d-wave pairing helps this issue.

In contrast to p-type materials, the kink effect is much weaker and basically not discernible along the nodal direction for n-type materials, fig. 2d²³, indicating a much weaker el-ph coupling. This significantly weakened effect is consistent with optical data, where the drop in $1/\tau$ is found to be much smaller in n-type material^{24,25}. Intuitively this is not surprising, as these high energy phonons must involve in-plane oxygen atoms, as suggested by dif-

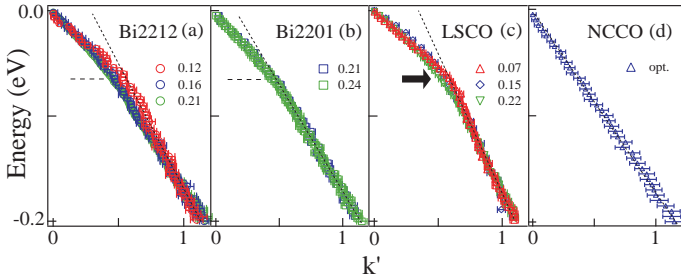


FIG. 2. The quasiparticle dispersions vs the rescaled momentum (k') are reported for three p-type materials systems; Bi2212 (panel a)^{14,16}, Bi2201 (panel b)¹⁶ and LSCO (panel c)¹⁶. The arrow indicates the frequency value obtained by inelastic neutron diffraction data. The dispersions are compared with the n-type superconductor NCCO (panel d)¹⁷ along ΓY . The rescaled momentum, k' , is defined as $(k - k_F)/k_{170\text{meV}}$. The dotted lines are guides to the eye and are obtained fitting the high energy part with a linear function.

ferent experiments²⁶. For p-type material the doped carrier predominately goes to the oxygen site, which can be the reason for the strong coupling. For n-type material, on the other hand, the doped carriers go to the copper site (upper Hubbard band), leading to weaker coupling.

A glance to Fig. 1a and Fig. 1b makes it clear that there is a correlation, as a function of doping, between the pairing gap size and the el-ph coupling constant. To first order, the most striking feature in both Fig. 1a and Fig. 1b is that the electron doped and hole doped materials are very different. The much weaker el-ph coupling strength explains smaller pairing gap in electron-doped material. Within a single band t-J or Hubbard model, one would expect particle hole symmetry. The other clear correlation is that the pairing strength of p-type material decreases with doping in Fig. 1a, as does the el-ph coupling constant in Fig. 1b. We believe that the correlation seen in these figures makes a strong case for the el-ph coupling being a key to pairing.

As for the systematic on the gap size in different p-type materials, other factors come in. It is known that the material dependent copper and apical oxygen distance correlates with T_c at optimal doping, T_c^{max} . Electronic structure analysis reduces this down to a correlation between T_c^{max} and the range of the intra-layer hopping²⁷. Hg1201 is found to have not only a larger intralayer hopping than LSCO/Bi2201, but also a larger interlayer hopping. The latter is due to the on-top stacking of the CuO_2 layers in Hg1201. In LSCO/Bi2201 the interlayer hopping is found to be substantially smaller due to the body-centered tetragonal stacking. Among other effects, an increased hopping reduces the Coulomb repulsion²⁷. We attribute the difference in μ^* being a key reason for maximum gap, Δ_{max} , to differ in different families of compounds. As we will elaborate, this is at least the likely reason for Δ in Bi2212/Hg1201 ($T_c^{max}=90\text{K}$) and LSCO/Bi2201 ($T_c^{max}=30\text{-}40\text{K}$) to segregate into two

groups. Hg1201 is found to have larger intra and interlayer hopping than LSCO/ Bi2201. For the much higher Δ_{max} in Hg1223 there is the additional possibility of higher phonon frequency. Optics experiment saw in fact a drop in $1/\tau$ in Hg1223 system at a frequency 30% higher than the one observed in Bi2212²⁸, which scales exactly with the pairing gap (and T_c) difference. A possible reason for this is the reduced strain on the CuO_2 sheets by other layers in this material.

We note a couple of issues with phonons. One reason why phonons are considered by many as unimportant is that the resistivity data do not show phonon signature in high temperature region. The second is that the data in Fig. 2 does not fit the simplest form of el-ph coupling mode. These unusual results are likely due to strong correlation effects and to the strong q dependence of the el-ph coupling in these materials. Both the non-Fermi liquid behavior and the el-ph coupling are needed to explain the data.

Fig. 3a shows the displacement pattern of the zone boundary half-breathing mode ($q=(\pi, 0)$), which corresponds to the important phonon with frequencies 50-80meV. There are several ways to consider its interaction with the electronic system. The usual approach is to consider the diagonal el-ph interaction in the particle number, namely the oxygen displacement is coupled to the electron density n_i in the i th Cu orbital²⁹. The in-plane oxygen displacement is pair-breaking for d-wave because it gives rise to the repulsive interaction between the electrons on the nearest neighbor Cu orbitals. This is more appropriate when the carriers are doped into the Cu orbital as in n-type cuprates, but not when they are doped into the oxygen orbital as in p-type cuprates. Further, the dielectric constant $\epsilon(\omega)$ at the energy of the gap $\omega = 2\Delta$ is much larger than one, and the repulsive interaction induced by the diagonal el-ph interaction is expected to be screened and reduced considerably.

For the holes, doped predominantly into the oxygen orbitals, there is an off-diagonal channel of el-ph interaction that is very important in cuprates. A realistic model of electronic structure is the d-p model, which considers the d- and p- orbitals as well as the strong Coulomb interactions. When we reduce the d-p model into the effective single-band t-J model, the transfer integral t_{ij} between the Zhang-Rice (ZR)³⁰ singlet states, at i and j sites, is given by the second order process in the hybridization $t_{pd} \sim 0.8\text{eV}$ between the d- and p-orbitals as

$$t_{ij} \cong \frac{t_{dp}^2}{\Delta_{dp}} \quad (2)$$

where Δ_{dp} is the energy difference between the p- and d-levels^{30,31}. In this expression the oxygen displacement modulates Δ_{dp} as $\Delta_{dp} = \Delta_0 - gu$, which leads to the off-diagonal el-ph interaction. Here Δ_0 is about 2eV, while g and u are the el-ph coupling constant and the displacement, respectively. The modulation of the transfer integrals t_{ij} , due to the motion of the oxygen at the

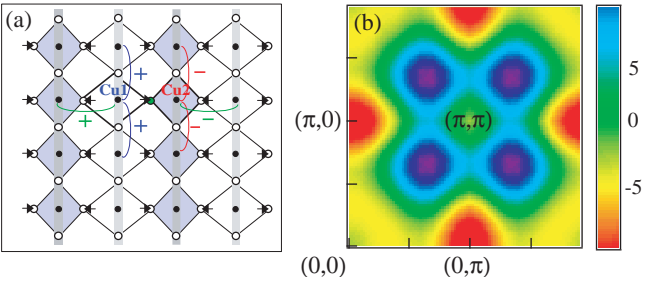


FIG. 3. In panel a) we report the displacement pattern of zone-boundary half-breathing mode of the CuO₂ planes. The black dots represent the Cu atoms, while the white one the oxygen atoms. The off-diagonal el-ph interaction are shown. The displacement of O at the center, modulates the energy of d-orbitals at the two Cu sites, Cu1 and Cu2. The effective transfer integral t_{ij} perpendicular to the displacements are modulated²⁰. In panel b) we report the contour plot of the momentum dependence of the pairing $e(q)$. Negative $e(q)$ indicates pair-creating region, while positive $e(q)$ indicates pair-breaking region. The pairing is zero (green) around the nodal region while it decrease gradually, reaching a minimum (red), approaching the $(\pi, 0)$ region.

center, changes the energy of the d-orbitals on Cu1 and Cu2 in the opposite direction, and hence modulates the six t_{ij} 's connected to Cu1 and Cu2 in the specified \pm pattern³² (as indicated by the sign of the bonds). By symmetry, the average shift of the two relevant Δ_{dp} 's modulates t_{ij} , and the transfer integral t_{12} on the center bond does not change. Taking other sites into account the modulation in t_{ij} , parallel to the displacement (green colored), cancel out and only the t_{ij} perpendicular to the displacements are modulated.

The above off-diagonal el-ph interaction, which is tied to the change of bond (rather than site) by lattice vibration, is significantly enhanced by the strong Coulomb interaction on the Cu site³³. As described below, this interaction creates d-wave pairing. Assuming the high frequency limit and integrating over the phonon coordinates with the off-diagonal el-ph interaction in Fig. 3(a), one obtains the effective el-el interaction Hamiltonian, H_{int} . We calculated the energy in the BCS approximation for d-wave superconductivity, with the order parameter $\Delta_k = \langle C_{k\uparrow} C_{-k\downarrow} \rangle = (\cos k_x - \cos k_y) / \sqrt{\cos^2 k_x + \cos^2 k_y}$ appropriate for the half-filled case. Then we obtain

$$\langle H_{\text{int}} \rangle_{BCS} \sim \sum_q g^2 \langle u_q u_{-q} \rangle e(q); \quad (3)$$

in Fig. 3(b) we show the contour plot of $e(q)$ ³⁴. It is found that the oxygen displacement contributes strongest to the d-wave pairing in exactly the region of q-space, namely near $q = (\pi, 0)$, where the strong coupling to the electrons is observed experimentally. In experiments, the anomalous dispersion of this half-breathing mode has been observed and the zone boundary region modes show the softening and couple to the electrons more strongly

than the zone center region modes²⁰. In another paper³⁵ it is found that el-ph coupling is strong from $(0.5\pi, 0)$ to $(\pi, 0)$. Integration of this range gives also pair creating results.

Therefore, certain phonon channels can be compatible with d-wave pairing. A detailed theory has to account for various channels, including the apical oxygen motion which is related to the phonon we consider. We hope that our discussion stimulates more theoretical investigations on the e-ph interaction in strongly correlated electron systems, as the data in Fig. 1 and Fig. 2 strongly suggest phonon to be a key player for superconductivity, independent of specific theory.

Fig. 4 proposes a phase diagram that contains essential ingredients for the key physics. At very high energy and temperature, there is an energy scale (or cross-over line) T_0 , which is related with J scale physics caused by strong Coulomb interactions. At lower energy scale (or temperature) phonons play an essential role in collaborating with antiferromagnetic interaction to deliver the pairing, yielding the intermediate pairing energy scale T_{phonon} (T_{ph}). This two scales energy scheme naturally explains the observation that there are two kinds of pseudogaps in underdoped cuprates, as strongly indicated by ARPES data near $(\pi, 0)$ ³⁶. The high energy one (hump) connects smoothly to that of the insulator³⁷. The low energy one (leading edge) is related to the superconducting gap³⁶.

A key issue for the classical phonon theory is the problem with μ^* . Since J has higher energy (fig. 4), the antiferromagnetic interaction dictates that the pairing state can only be of d-wave symmetry. This suppresses the s-wave pairing instabilities of some phonons while cooperates with the d-wave pairing processes of other phonons. Since the d-wave state has a node at the origin, this significantly reduces the μ^* problem, because there is no amplitude on the same site, and the on-site repulsion is not an issue. We note that while μ^* in (1) is introduced in the context of s-wave superconductor, the μ^* in the discussion here should be the repulsive interaction on the neighboring orbitals for a d-wave state, which is expected to be reduced by the strong $\epsilon(\omega)$ screening. Given the importance of phonons, we believe that it is reasonable to make discussion in parallel of equation (1), although the way phonons come in and the pairing symmetry are different. Another critical role of the strong Coulomb interaction is that it significantly enhances the off-diagonal el-ph coupling near the quasi-resonance of the p- and d-levels of cuprates³³. As we have indicated earlier, the high phonon frequency of 50-80meV and the strong coupling constant can deliver a pairing strength that is an order of magnitude higher (and thus high- T_c) if the μ^* problem can be significantly reduced.

While significantly reduced μ^* , nevertheless is likely the reason for Δ_{max} to vary among families of compounds. Aside from theory²⁷, that is based on the average structural data, this tendency is re-enforced by local structural data. As shown by local structural probes,

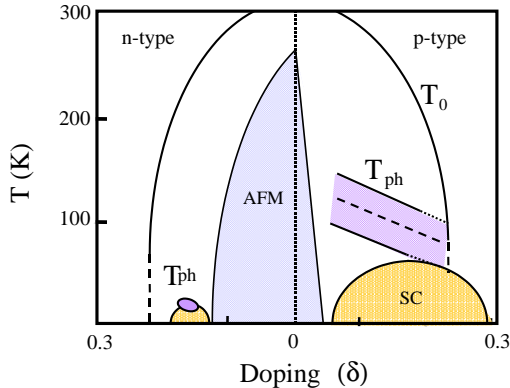


FIG. 4. A schematic phase diagram for high temperature materials is presented. The black line represent the T_0 line, which is particle-hole symmetric in the t-J model. The purple shaded area represents the range where the phonons become important. The superconducting regime (SC) is indicated by yellow shaded area and the antiferromagnetic regime (AF) by blue shaded area.

the 70meV zone boundary phonon couples with dynamic local structural distortions²⁶. While the size of the distortions in LSCO and Bi2212/YBCO are comparable, the onset temperatures of the distortion (T^*) is significantly lower in LSCO, likely related to stripes³⁸. This coupling with more static structural distortion in LSCO lowers the conductivity and screening of μ^* , and thus explains the lower value of Δ_{max} , although ω_0 or λ' are comparable. For a similar reason we do not observe any clear change of ω_0 or λ' in the $\text{La}_{1.28}\text{Nd}_{0.6}\text{Sr}_{0.12}\text{CuO}_4$ (NdLSCO) system with respect to optimally doped LSCO³⁹. The stripes and distortion in NdLSCO are static, further suppressing pairing.

The above interpretation receives support from the huge change in T^* (order of 80K) with isotope substitution⁴⁰. The opposite change in the T^* respect to the one in the T_c (T^* increases with increasing the mass of the isotope), is consistent with the idea that more static lattice distortions suppress pairing. The local structural distortion is likely to be similar in Bi2201 and this may explain why the maximum T_c (30K) for the single layer is much lower than that of the isostructural single layer of Tl and Hg compounds. The difference in the dynamics of local structural distortion between different families and different dopings is probably related to the mismatch between the CuO_2 plane and the block layers⁴⁰⁻⁴². As one introduces more CuO_2 planes in a unit cell, their structures are less vulnerable to strains from other layers, and this may explain why T_c increases with number of layers in Bi, Tl and Hg based families of cuprates.

We now briefly discuss the connection between the picture which emerges here and those in the literature. Obviously, phase diagrams similar to Fig. 4 already exist, except that the data in Fig. 1a and Fig. 1b

strongly suggest that the intermediate pairing line is associated with phonons. In the case without charge ordering, both the weak coupling spin-fluctuation theory^{43,44} and strong coupling theories based on Hubbard or t-J models⁴⁵ have been extensively studied. In these cases, the antiferromagnetic correlation effect is the only ingredient considered, without including phonon effects. For strong coupling theories there is no consensus on the lowest energy state in these strongly coupled models, with flux phase, d-wave pairing, and anti-ferromagnetically ordered ground states being possible candidates. Naturally, a possible ground state is a linear combination or the fluctuating state among them⁴⁶. A way to view the effect of phonons is that it helps to stabilize the d-wave pairing state among the competing ground states. Unfortunately, similar theoretical analysis, like those in Fig. 4 show that phonon helps all these states. Alternatively, it is also possible that antiferromagnetic interaction alone provides weak d-wave pairing^{43,44}, but it is the phonon that enhances it.

Next is the case where one considers the additional instabilities of charge ordering (stripes) or charge-density waves⁴⁷. These models are related to what we propose, since the stripe approach also includes two energy scales. In some theories phonons are considered, while in others only the electronic degrees of freedom are stressed⁴⁸. For the cases involving the Hubbard-Holstein model, the discussion mainly concentrates on the issue of quantum critical points without specifying the role of these particular phonons⁴⁹. For the cases where only the electronic aspects of the stripes are considered, the two energy scales correspond to the scales when the stripes and pairs are formed respectively⁵⁰. In this case the pairing of the carriers is purely electronic, driven by quasi-1D behavior. Independently of the specifics, it would be interesting to see the role of the electronic stripes on the el-ph coupling considered in our case. Naturally, charge ordering couples to lattice distortions. The fact that the el-ph coupling is strong for phonons with q value from $(0.5\pi, 0)$ to $(\pi, 0)$ could be interpreted as the system tendency to couple with stripes of 4a to 2a periodicities³⁵. This issue of coupling to 2a periodicity has been discussed before⁵¹. As shown in Fig. 3, the $(\pi, 0)$ phonon has a clear 1D character with 2a periodicity. This could be regarded as the instantaneous creation of the dynamic stripes because the charge should be accumulated/diluted alternatively along the Cu-O chain perpendicular to the displacement. Alternatively, one can say that the systems tendency to have stripes will promote el-ph coupling with desired q , that is pair creating for d-wave state. Before leaving the subject of theory, we also note that there are extensive work on phonons only, without explicit consideration of the strong Coulomb correlation, notably the polaronic effect⁵². Here we think that the d-wave aspects are important because of the μ^* problem.

Whatever the specific relationship between our finding and the interesting theoretical ideas discussed above may be, the data hint strongly that the el-ph interaction

must be considered explicitly. At the same time, we also stress that the el-ph interaction must be considered in the context of strong electronic correlation, as the t-J model has been remarkably successful to describe the electronic structure of cuprates down to J scale^{2,45}. In this sense the strongly correlated t-J model does provide a basis for cuprate physics, with phonons add to it in delivering d-wave superconductivity with very high- T_c .

In summary, we have shown a comparison of photoemission experiments in conjunction with neutron, optics and local structural probes, providing direct evidence for strong el-ph coupling being important for pairing. The inclusion of el-ph interaction explains many experimental observations that cannot be understood by strongly interacting models of CuO_2 planes alone.

We would like to acknowledge P. V. Bogdanov, X. J. Zhou and S. A. Keller for experimental help. We would like to thank T. H. Geballe, S. Doniach, D. H. Lee, R. B. Laughlin, S. A. Kivelson, P. Allen and D. Bonn for useful discussion. The SSRL's work was supported by the DOE, Office of Basic Energy Science, Division of Materials Science. The work at ALS was supported by the Office of Division of Materials Science with contract DE-AC0376SF00098. One of us A.L. would like to thank the Instituto Nazionale Fisica della Materia (INFM).

¹ P. W. Anderson Science **235**, 1196 (1987)

² Z. X. Shen and G. A. Sawatzky, Phys. Status Solidi B **215**, 523 (1999); and references therein

³ H. Fukuyama Journal of Magnetism and Magnetic Materials **54-57**, 1437 (1986)

⁴ G. Kotliar and J. Liu, Phys. Rev. B **38**, 5142 (1988)

⁵ B. Battlogg in *High Temperature Superconductivity*, K. S. Bedell *et al.* eds. (Addison-Wesley, Reading, MA, 1990)

⁶ P. W. Anderson *The Theory Of Superconductivity In The High- T_c Cuprates* (Princeton, N.J. : Princeton University Press, (1997)

⁷ *International Conference on Stripes, Lattice Instabilities, and High T_c Superconductivity*, edited by A. Bianconi and N. L. Saini J. Supercond. **10**, no.4 (1997); *Lattice effect in High T_c superconductors* edited by Y. Bar-Yam, T. Egami, J. Mustre de Leon and A. R. Bishop (World Scientific, Singapore 1992)

⁸ J. G. Bednorz and K. A. Muller, Z. Phys. B **64**, 189 (1987)

⁹ S. Doniach and M. Inui Phys. Rev. B **41**, 6668 (1990)

¹⁰ Y. J. Uemura Phys. Rev. Lett **66**, 2665 (1991)

¹¹ V. J. Emery and S. A. Kivelson, Phys. Rev. Lett **74**, 3253 (1995)

¹² D. J. Scalapino, in *Superconductivity* edited by R.D.Parks (Marcel Dekker, New York , 1969) pp449 Vol.I, and references therein.

¹³ T. Valla *et al.*, Phys. Rev. Lett. **83**, 2085 (1999)

¹⁴ P. V. Bogdanov *et al.* Phys. Rev. Lett. **85**, 2581 (2000)

¹⁵ A. Kaminski *et al.* cond-mat 0004482 (2000)

¹⁶ A. Lanzara *et al.* preprint

¹⁷ N. P. Armitage, M. Greven, P. Mang *et al.* preprint

¹⁸ T. Timusk *et al.* Reports on Progress in Physics, IOP Publishing **62**, 61-122 (1999)

¹⁹ M. Eschrig, M. R. Norman Phys. Rev. Lett. **85**, 3261 (2000); A. Kaminski *et al.* cond-mat 0004482 (2000)

²⁰ R. J. McQueeney *et al.*, Phys. Rev. Lett. **82**, 628 (1999); Y. Petrov *et al.* cond-mat0003414 (2000)

²¹ M. R. Norman and H. Ding Phys. Rev. B **57**, R11089 (1998)

²² N. W. Ashcroft and N. D. Mermin in *Solid State Physics*, Holt, Rinehart and Winston, New York pp. 519 (1976); Here we make a distinction between the el-ph coupling constant λ' determined in this way and the λ used in strong coupling theory. In the limit of weak coupling λ and λ' are equal.

²³ The kink effect is basically none existing along the nodal direction, and the effect is stronger in other directions.

²⁴ D. N. Basov *et al.* preprint

²⁵ P. Calvani *et al.* Phys. Rev. B **53**, 2756 (1996)

²⁶ A. Bianconi, M. Missori, State Commun. **91**, 1 (1994); Phys. Rev. Lett. **76**, 3412 (1996); K. A. Muller J. Superconductivity **12**, 3 (1999); S. J. Billinge Phys. Rev. Lett. **72**, 2282 (1994); H. A. Mook Nature **401**, 145 (1999)

²⁷ E. Pavarini *et al.* cond-mat 0012051

²⁸ J. J. McGuire *et al.* Phys. Rev. B **62**, 8711 (2000)

²⁹ N. Bulut and D. J. Scalapino Phys. Rev. B **54**, 14971 (1996)

³⁰ F. C. Zhang and T. M. Rice, Phys. Rev. B **37**, 3759 (1988)

³¹ Y. Ohta, T. Tohyama, and S. Maekawa, Phys. Rev. Lett. **66**, 1228 (1991)

³² It has been pointed out first by J. Lorenzana and G.A.Sawatzky (Phys. Rev. Lett. **74**, 1867 (1995)) that the effective spin-exchange interaction J_{dd} between the two neighboring Cu orbitals are modulated by the oxygen displacement.

³³ S. Ishihara, T. Egami, and M. Tachiki, Phys. Rev. B **55**, 3163 (1997)

³⁴ N. Nagaosa, in preparation

³⁵ L. Pintschovius and M. Braden, Phys. Rev. B **60**, R15039 (1999)

³⁶ D. S. Marshall *et al.* Phys. Rev. Lett **76**, 4841 (1996)

³⁷ R. B. Laughlin Phys. Rev. Lett. **79**, 1726 (1997)

³⁸ J. M. Tranquada *et al.* Nature **375**, 561 (1995); Phys. Rev. B **59**, 14712 (1999); K. Yamada *et al.* Phys. Rev. B **57**, 6165 (1998)

³⁹ X. J. Zhou *et al.* cond-mat 0009002

⁴⁰ A. Lanzara *et al.* J. Phys. Condens Mat. **11**, L541 (1999); M. Medarde *et al.* Phys. Rev. Lett **16**, 2397 (1998)

⁴¹ A. Bianconi *et al.* International Journal of Modern Physics B. vol. XX (2000); and reference therein.

⁴² P. Bordet *et al.* Physica C **282**, 1081 (1997); A. Lanzara *et al.* Phys. Rev. B **59**, 3851 (1999); N. L. Saini *et al.* J. Phys. IV **7**, 1245 (1997)

⁴³ D. J. Scalapino Physics Report **250** n.6, 329 (1995)

⁴⁴ A. Sokol and D. Pines Phys. Rev. Lett **71**, 2813-2816 (1993)

⁴⁵ see for example F. Gebhard in *The Mott Metal-Insulator Transition*, (Springer, 1997); M. Imada, A. Fujimori, and Y. Tokura, Rev. Mod. Phys. **70**, 1039 (1998)

⁴⁶ X.-G. Wen and P. A. Lee Phys. Rev. Lett. **76**, 503 (1996); **80**, 2193 (1998). P. Lee, N. Nagaosa, T.K. Ng, and X.G.

Wen, Phys. Rev. B **57**, 6003 (1998).

⁴⁷ J. Zaanen and O. Gunnarson, Phys. Rev. B **40**, 7391 (1989); D. Poilbanc and T. M. Rice, Phys. Rev. B **39**, 9749 (1989); C. Castellani *et al.* Phys. Rev. Lett. **75**, 4650 (1995); A. H. Castro Neto and D. Hone Phys. Rev. Lett. **76**, 2165 (1996); C. Morai Smith *et al.* Phys. Rev. Lett. **58**, 453 (1998); S. A. Kivelson *et al.* Nature **393**, 550 (1998); S. A. Kivelson and V. J. Emery in *Strongly Correlated Electronic Materials: The Los Alamos Symposium 1993*, edited by K. S. Bedell *et al.* (Addison-Wesley, Reading, MA, 1994), pp. 619-650; S. R. White and D. J. Scalapino, Phys. Rev. Lett **80**, 1272 (1998)

⁴⁸ B. K. Chakraverty, J. Phys. **42**, 1351 (1981); A. R. Bishop *et al.* Z. Phys. B **76**, 17 (1989); J. B. Goodenough and J. Zhou Phys. Rev. B **42**, 4276 (1990); K. Yonemitsu, A. R. Bishop and J. Lorenzana Phys. Rev. Lett. **69**, 1600 (1992); H. Roder *et al.* Phys. Rev. Lett. **70**, 3498 (1993)

⁴⁹ M. Grilli and C. Castellani, Phys. Rev. B **50**, 16880 (1994); M. L. Kulic and R. Zeyher, Phys. Rev. B **49**, 4395 (1994); K. J. von Szczepanski and K. W. Becker, Z. Phys. B **89**, 327 (1992)

⁵⁰ V. J. Emery, S. A. Kivelson and O. Zachar, Phys. Rev. B **56**, 6120 (1997)

⁵¹ N. Reed and S. Sachdev Phys. Rev. Lett **62**, 1694 (1989)

⁵² B. K. Chakraverty, J. Phys. **42**, 1351 (1981); A. Alexandrov and J. Ranninger **23**, 1796 (1981); A. S. Alexandrov *et al.*, Phys. Rev. Lett. **56**, 949 (1986); R. Micnas, J. Ranninger and S. Robaszkiewicz, Rev. Mod. Phys. **62**, 113 (1990)

⁵³ For photoemission data on LSCO (blue full circles) see A. Fujimori *et al.* cond-mat 0011293 (2000); Bi2212 see H. Ding *et al.* cond-mat 0006143 (2000) (full triangles); D. L. Feng *et al.*, Science **289**, 277 (2000) (full red squares); A. Lanzara *et al.* preprint (full reversed triangles, triangles and circles); on the left side of the panel, NCCO see N. P. Armitage *et al.*, cond-mat 0012003, to be published in Phys. Rev. Lett.

⁵⁴ For tunneling data on LSCO (empty blue circles and triangles) see T. Nakano *et al.* J. Phys. Soc. Jpn; Bi2212 see Y. De Wilde *et al.*, Phys. Rev. Lett. **80**, 153 (1998) (red empty square); N. Miyakawa *et al.*, Phys. Rev. Lett. **80**, 157 (1998) (red empty triangles); and C. H. Renner *et al.*, Phys. Rev. Lett. **80**, 149 (1998); *ibid.* **80**, 3606 (1998) (red empty circle); Hg1223 (full black squares) and Hg1201 (full black circles) see C. Panagopoulos *et al.*, Phys. Rev. Lett. **79**, 2320 (1997). On the left side of the phase diagram, for NCCO see Q. Huang *et al.*, Nature **347**, 309 (1990) and S. Kashiwaya *et al.*, Phys. Rev. B **57**, 8680 (1998)

⁵⁵ For transport data on Hg1223 (black circles) see A. Fukuoka *et al.*, Phys. Rev. B **55** 6612 (1997); for Bi2212 (red circles) see A. Maeda *et al.*, Phys. Rev. B **41**, 6418 (1990); for Bi2201 (grey circles) see A. Maeda *et al.*, Phys. Rev. B **41**, 4112 (1990); for LSCO (blue circles) see H. Takagi *et al.*, Phys. Rev. B **40**, 2254 (1989); for NCCO (green circle) see Y. Tokura *et al.*, Nature **337**, 345 (1989); H. Takagi *et al.*, Phys. Rev. Lett. **62**, 1197 (1989)